Improved visible-light triggered photocatalytic activities of BiOCl microplates via synergistic effect of doping and heterojunction engineering

Qian Wu[a], Xiaoqing Lai[a], Xiao-Hui Ji[b], Hai Jiang[a]*, Peng Du[a]*

[a]*Department of Microelectronic Science and Engineering, School of Physical Science and Technology, Ningbo University, 315211 Ningbo, Zhejiang, China*

[b]*Shaanxi Province Key Laboratory of Catalysis, College of Chemical & Environment Science, Shaanxi University of Technology, Hanzhong 723001, P.R. China*

Corresponding authors

E-mail: jianghai@nbu.edu.cn (H. Jiang); dp2007good@sina.com or dupeng@nbu.edu.cn (P. Du)

Preparation of Sm^{3+}-doped BiOCl microplates

$Bi_{1-x}OCl:xSm^{3+}$ ($BiOCl:xSm^{3+}$; $0 \leq x \leq 0.05$) microplates were synthesized through high-temperature solid-state reaction method. Herein, Bi_2O_3, NH_4Cl and Sm_2O_3 were used as the raw materials. These raw materials were weighted according to the stoichiometric ratio. Note that, to make up the loss of volatilization, excess 20% of NH_4Cl was added. The weighed raw materials were thoroughly mixed for 30 min via an agate mortar. After that, they were sintered at 673 K for 3 hours in a furnace. When the sintering process was finished, white powders were obtained and collected for further characterization.

Synthesis of g-C_3N_4

To synthesize the g-C_3N_4, a conventional high-temperature solid-state reaction method was used. In brief, 2 g of melamine was weighed and placed in a crucible, and then heated at 823 K for 5 h in a furnace. After that, the g-C_3N_4 was prepared.

Sample characterization

X-ray diffractometer (Bruker D8 Advance; Cu *Kα* irradiation), UV-vis spectrophotometer (Cary 5000), field-emission scanning electron microscopy (FE-

SEM, Hitachi SU-70) and a multifunctional imaging electron spectrometer (Thermo ESCALAB 250XI) were utilized to investigate the phase structure, microstructure, light absorption capacity and elemental compositions of final products, respectively. The Raman spectra of the prepared samples were tested by a microfluorescence spectrometry system (Ocean Optics QE pro). The luminescence properties of studied samples were examined through a fluorescence spectrometer (Edinburgh FS5). The electron paramagnetic resonance (EPR) spectrum of oxygen vacancy was recorded on a Bruker EMXplus A300 spectrometer.

Table S1. Calculated lattice parameters of BiOCl, BiOCl:0.005Sm^{3+} and BiOCl:0.010Sm^{3+} microplates via Rietveld XRD refinement.

Parameters	BiOCl	BiOCl:0.005Sm^{3+}	BiOCl:0.010Sm^{3+}
a (Å)	3.8928	3.8926	3.8916
b (Å)	3.8928	3.8926	3.8916
c (Å)	7.3690	7.3667	7.3636
V (Å^3)	111.67	111.62	111.52
$\alpha = \beta = \gamma$	90°	90°	90°
R_p	0.0867	0.0922	0.0846
R_{wp}	0.1304	0.1295	0.1241
χ^2	1.973	2.275	1.922

Table S2. *K* values of BiOCl:*x*Sm^{3+} microplates under visible light irradiation.

Compounds	*K* (min^{-1})
BiOCl	0.00096
BiOCl:0.003Sm^{3+}	0.00109
BiOCl:0.005Sm^{3+}	0.00154
BiOCl:0.008Sm^{3+}	0.00135
BiOCl:0.010Sm^{3+}	0.00145
BiOCl:0.030Sm^{3+}	0.00130
BiOCl:0.050Sm^{3+}	0.00106

Table S3. *K* values of BiOCl:Sm^{3+}@*y*g-C_3N_4 heterojunction composites excited by visible light.

Compounds	*K* (min^{-1})
g-C_3N_4	0.00336
BiOCl:Sm^{3+}	0.00154
BiOCl:Sm^{3+}@5%g-C_3N_4	0.00214
BiOCl:Sm^{3+}@10%g-C_3N_4	0.00266
BiOCl:Sm^{3+}@20%g-C_3N_4	0.00379
BiOCl:Sm^{3+}@30%g-C_3N_4	0.00449
BiOCl:Sm^{3+}@40%g-C_3N_4	0.00524
BiOCl:Sm^{3+}@50%g-C_3N_4	0.00568
BiOCl:Sm^{3+}@60%g-C_3N_4	0.00664

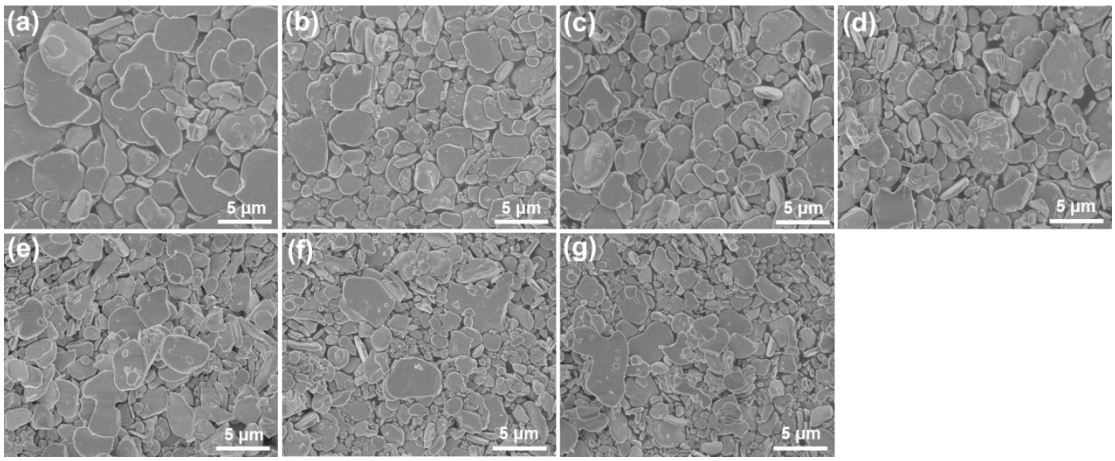

Figure S1 FE-SEM images BiOCl:xSm^{3+} compounds with the Sm^{3+} contents of (a) x = 0.000, (b) x = 0.003, (c) x = 0.005, (d) x = 0.008, (e) x = 0.010, (f) x = 0.030 and (g) x = 0.050.

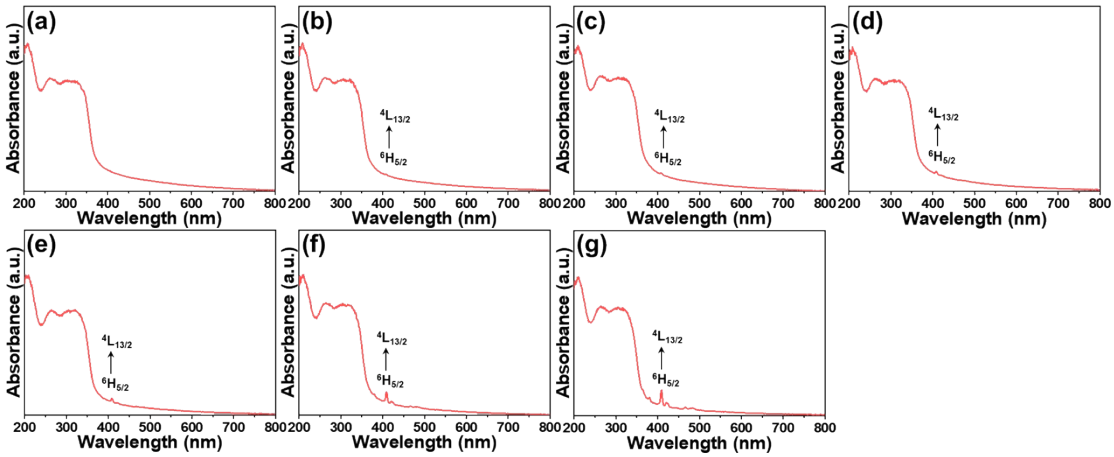

Figure S2 UV-Vis absorption spectra of BiOCl:xSm^{3+} microplates with different Sm^{3+} contents of (a) x = 0.00, (b) x = 0.003, (c) x = 0.005, (d) x = 0.008, (e) x = 0.010, (f) x = 0.030 and (g) x = 0.050.

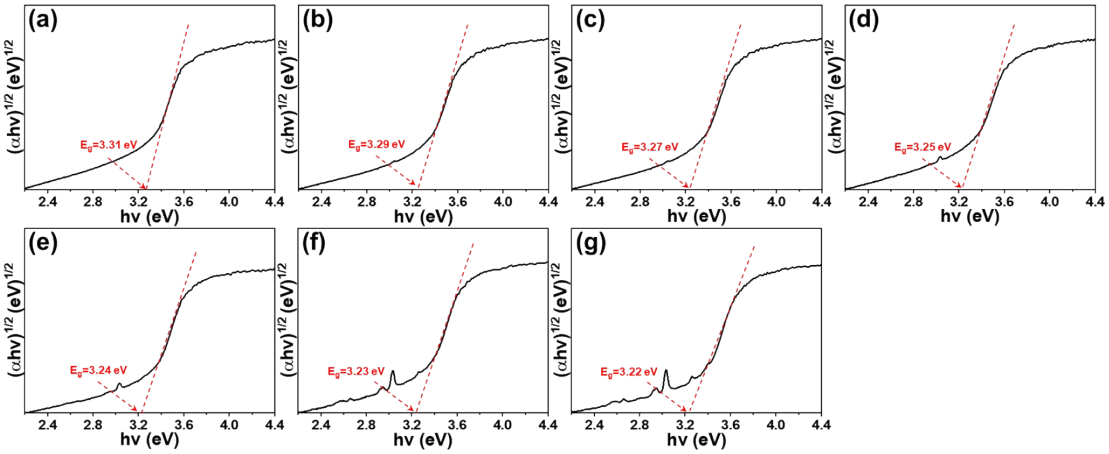

Figure S3 Evaluation of E_g values of BiOCl:xSm^{3+} microplates with different Sm^{3+} concentrations of (a) x = 0.00, (b) x = 0.003, (c) x = 0.005, (d) x = 0.008, (e) x = 0.010, (f) x = 0.030 and (g) x = 0.050 by Kubelka-Munk function.

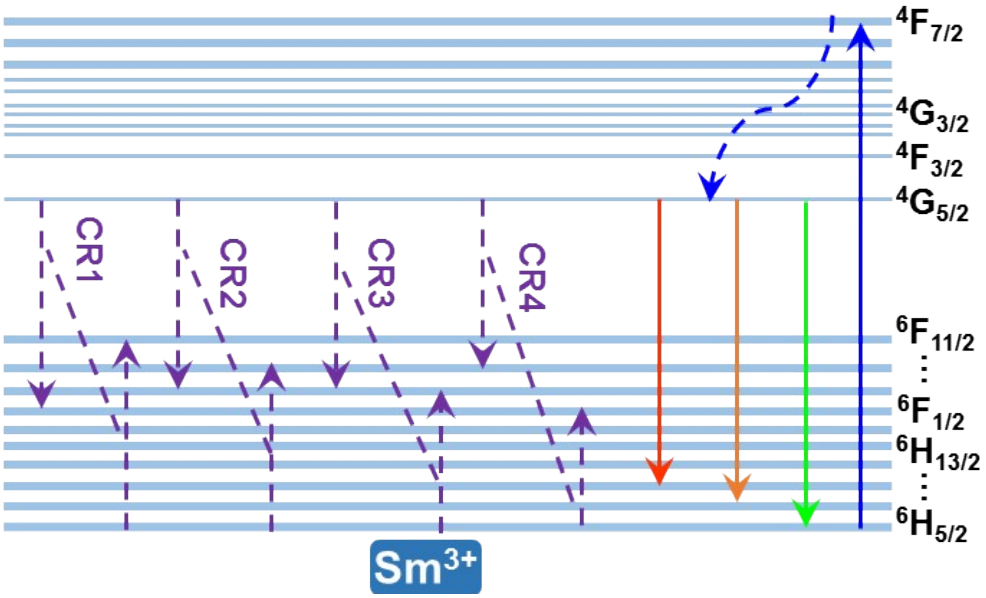

Figure S4 Energy level diagram of Sm^{3+} in BiOCl host lattices.

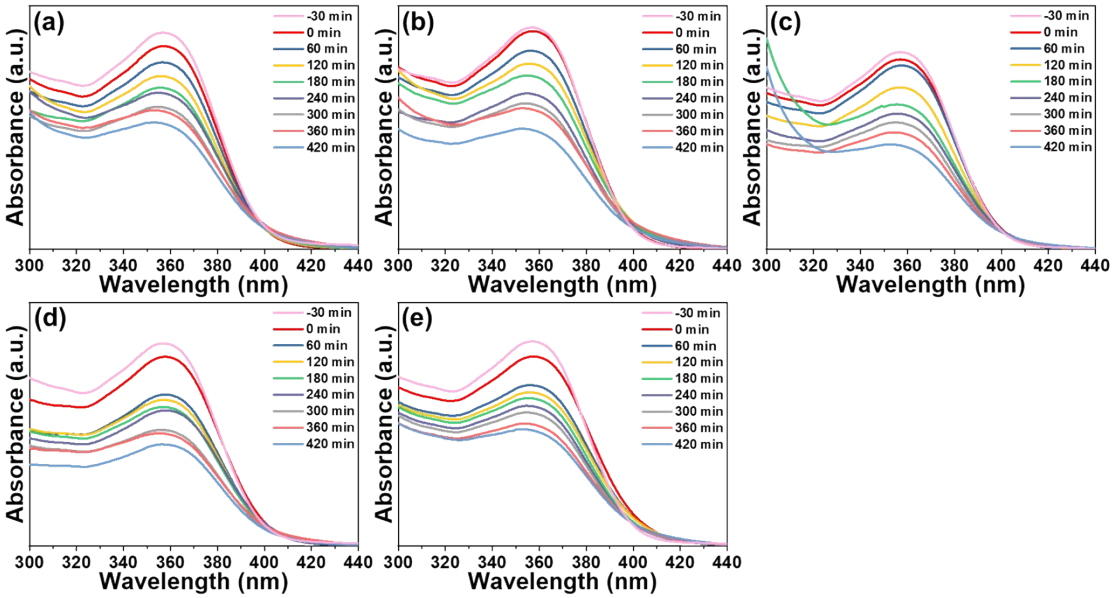

Figure S5 The UV-vis absorption spectra of TC degradation with BiOCl:xSm^{3+} microplates doped with different Sm^{3+} contents of (a) x =0.003, (b) x = 0.008, (c) x = 0.010, (d) x = 0.030 and (e) x = 0.050.

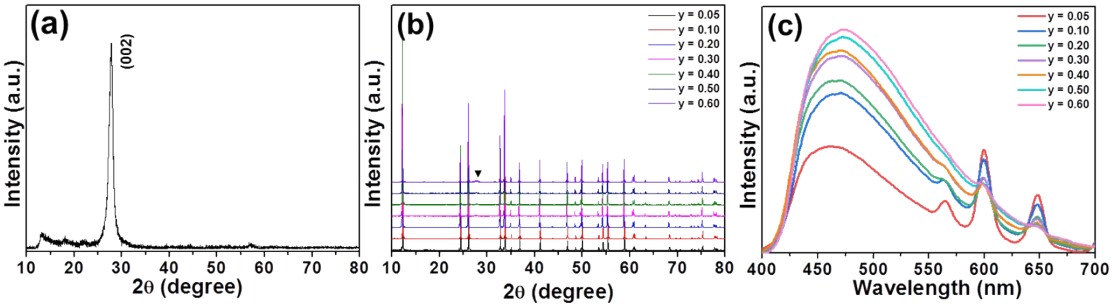

Figure S6 (a) XRD pattern of the g-C_3N_4. (b) XRD patterns and (c) Emission spectra of BiOCl:Sm^{3+}@*y*g-C_3N_4 heterojunction composites excited at 365 nm.

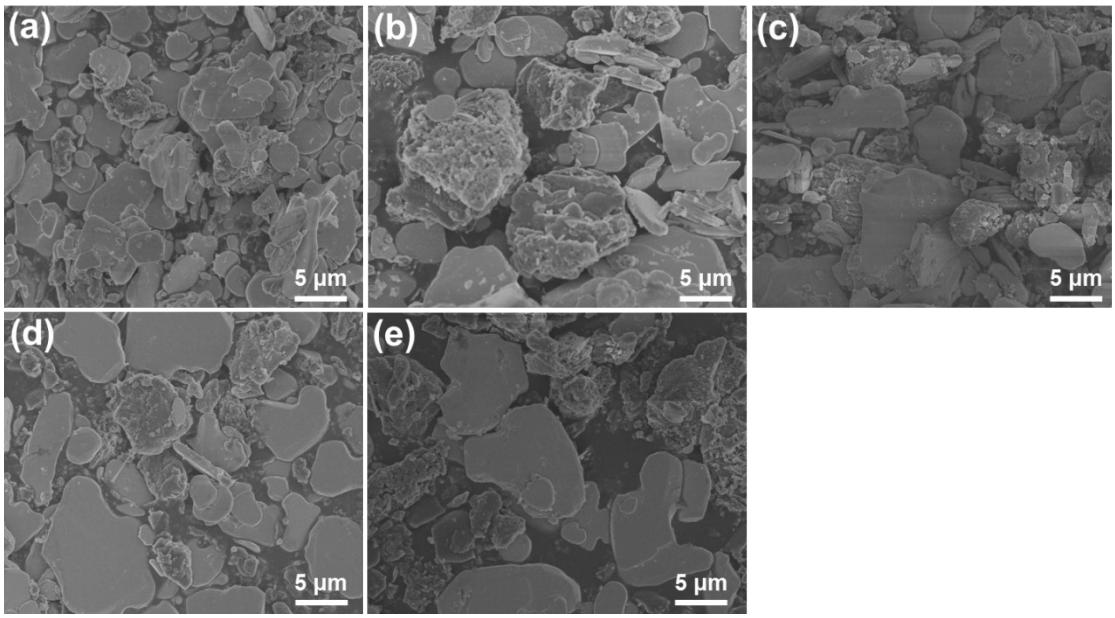

Figure S7 FE-SEM images of the BiOCl:Sm^{3+}@*y*g-C_3N_4 heterojunction composites with different weight percentages of (a) *y* = 10%, (b) *y* = 20%, (c) *y* = 30%, (d) *y* = 40% and (e) *y* = 50%.

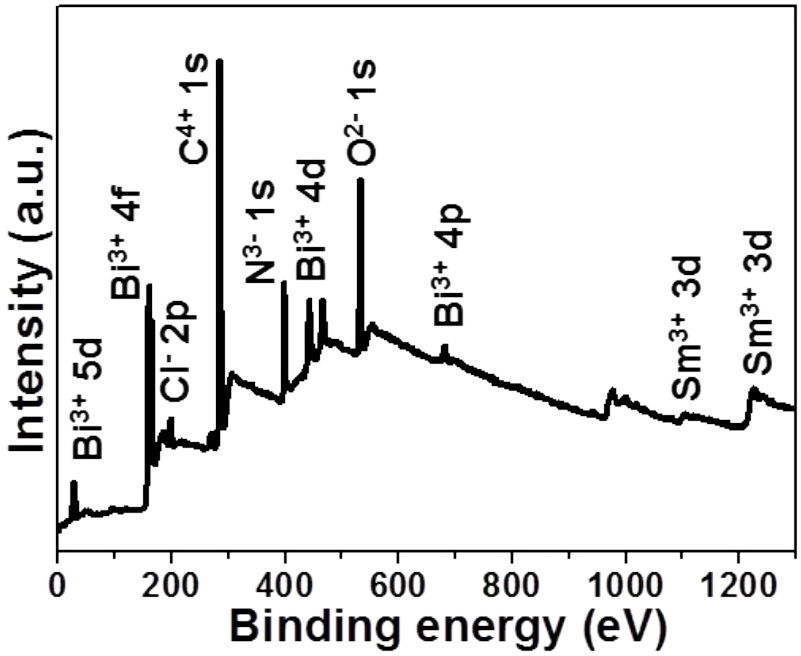

Figure S8 XPS survey spectrum of BiOCl:Sm^{3+}@60%g-C_3N_4 heterojunction composites.

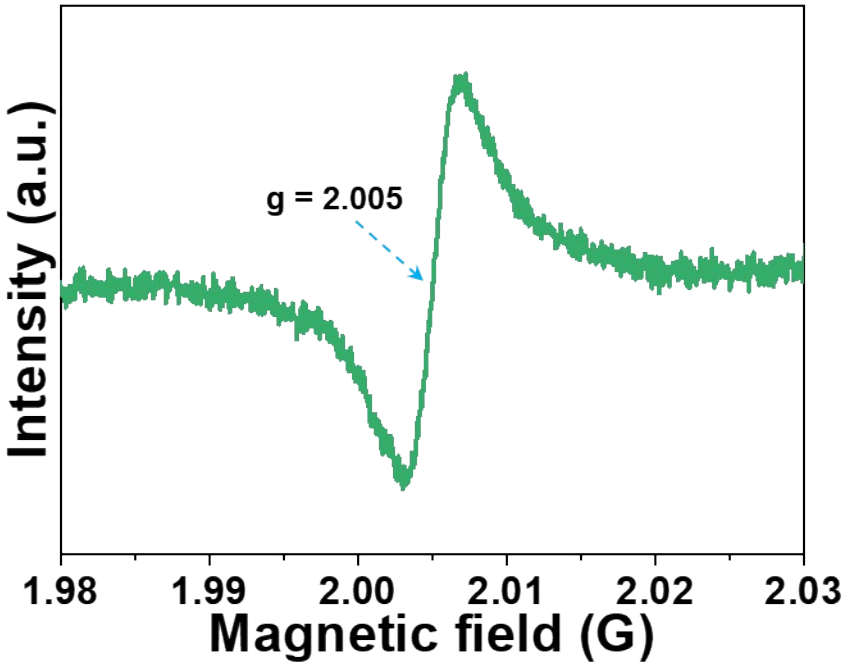

Figure S9 EPR spectrum of BiOCl:0.010Sm^{3+} microplates at room temperature.

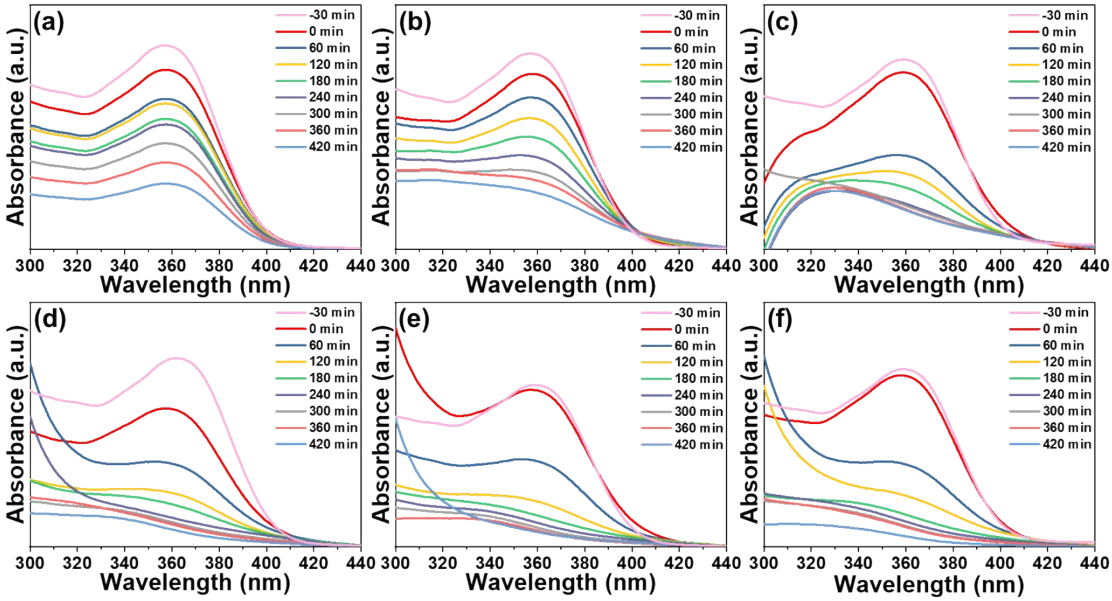

Figure S10 The UV-vis absorption spectra of TC degradation in the presence of BiOCl:Sm^{3+}@*y*g-C_3N_4 heterojunction composites with diverse g-C_3N_4 contents of (a) *y* =5%, (b) *y* = 10%, (c) *y* = 20%, (d) *y* = 30% (e) *y* = 40%, and (f) *y* = 50%.

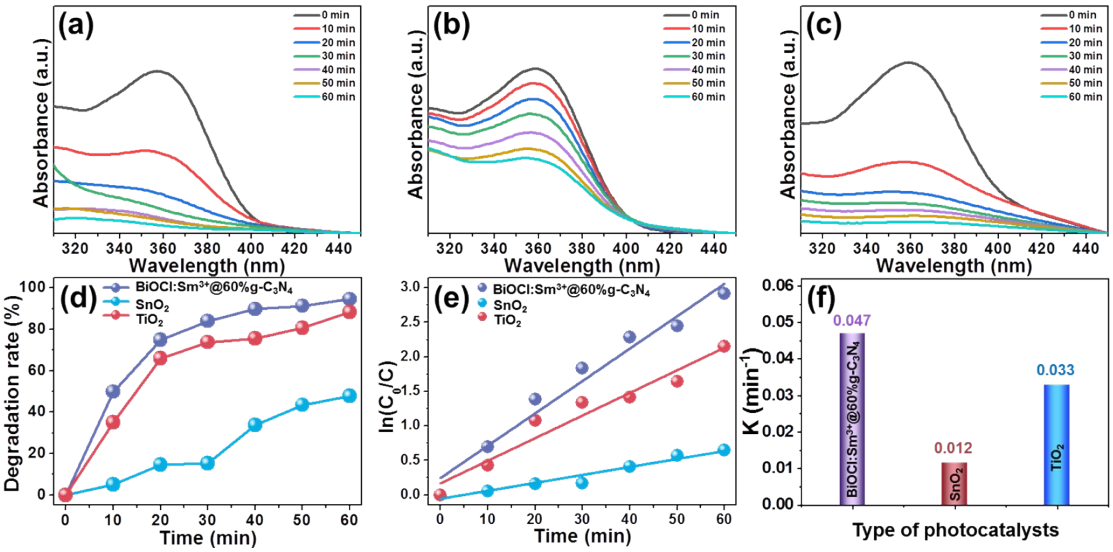

Figure S11 UV-vis absorption spectra of TC degradation via using (a) commercial SnO_2 (b) commercial TiO_2 and (c) BiOCl:Sm^{3+}@60%g-C_3N_4 heterojunction composites. (d) Degradation rates of TC by commercial SnO_2, TiO_2 and BiOCl:Sm^{3+}@60%g-C_3N_4 heterojunction composites under full-spectrum light irradiation. (e) Plots of the $\ln(C_0/C)$ versus time t for the related photocatalysts. (f) Kinetic rates of TC degradation via using the related photocatalysts under full-spectrum light irradiation.

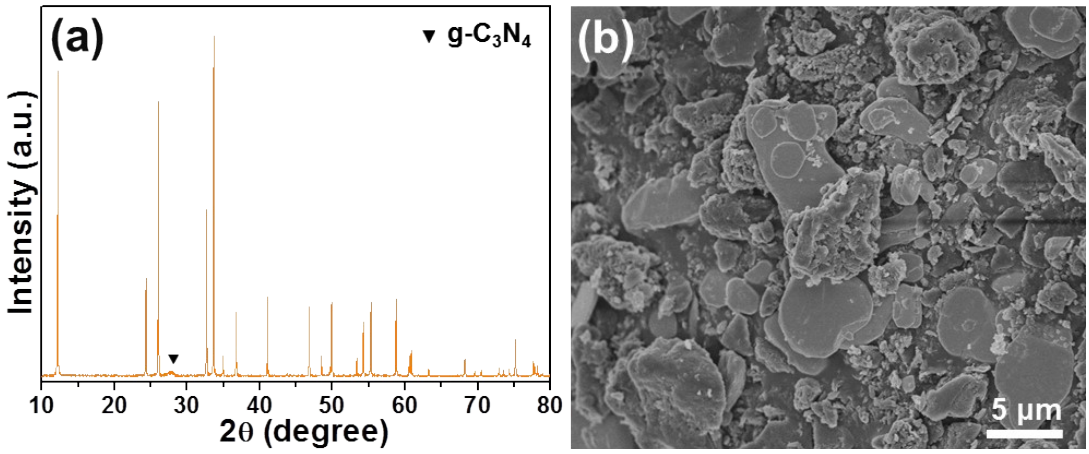

Figure S12 (a) XRD pattern and (b) FE-SEM image of BiOCl:Sm^{3+}@60%g-C_3N_4 heterojunction composites after cyclic experiment.

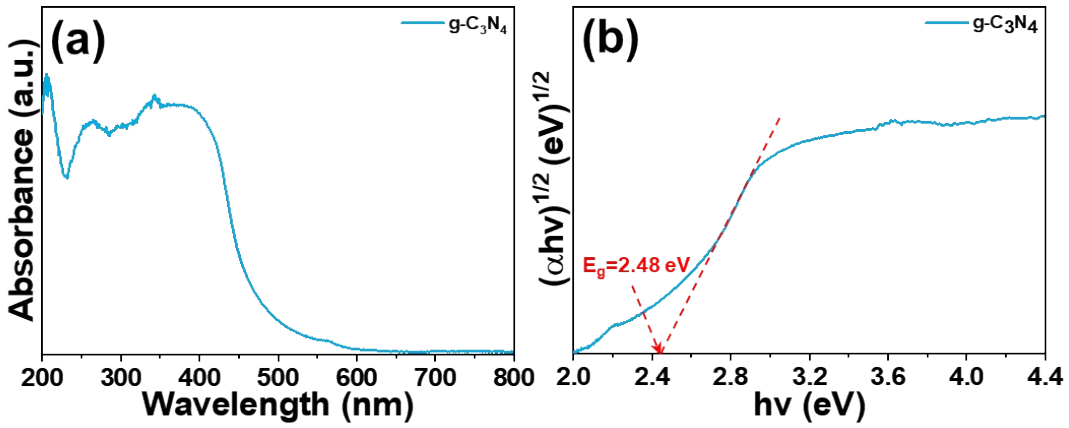

Figure S13 (a) UV-vis absorption spectrum of g-C_3N_4. (b) Evaluation of E_g values of g-C_3N_4 by Kubelka-Munk function.

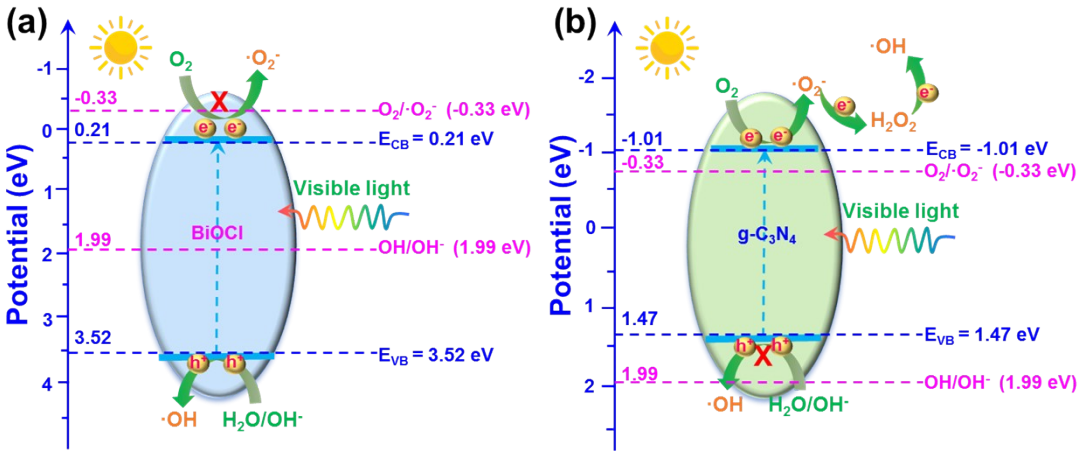

Figure S14 Band positions of (a) BiOCl and (b) g-C_3N_4.

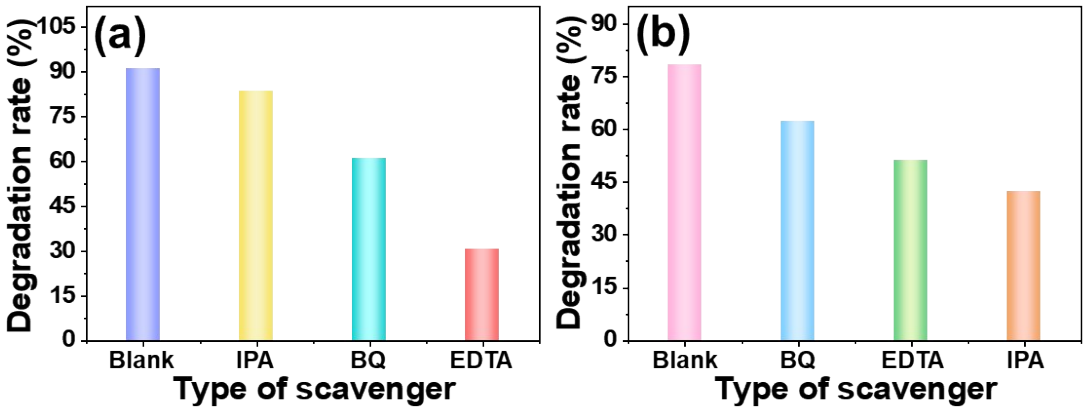

Figure S15 Trapping experiments of the active species for TC degradation by utilizing of (a) BiOCl:0.005Sm^{3+} microplates and (b) g-C_3N_4.